Curcumin nanoparticles containing poloxamer or soluplus tailored by high pressure homogenization using antisolvent crystallization

Article (Accepted Version)

Curcumin nanoparticles containing poloxamer or soluplus tailored by high pressure homogenization using antisolvent crystallization

Alireza Homayouni, Marjan Amini, Masoumeh Sohrabi, Jaleh Varshosaz, Ali Nokhodchi

PII: S0378-5173(19)30224-8
DOI: https://doi.org/10.1016/j.ijpharm.2019.03.038
Reference: IJP 18222

To appear in: *International Journal of Pharmaceutics*

Received Date: 5 November 2018
Revised Date: 16 March 2019
Accepted Date: 18 March 2019

Please cite this article as: A. Homayouni, M. Amini, M. Sohrabi, J. Varshosaz, A. Nokhodchi, Curcumin nanoparticles containing poloxamer or soluplus tailored by high pressure homogenization using antisolvent crystallization, *International Journal of Pharmaceutics* (2019), doi: https://doi.org/10.1016/j.ijpharm.2019.03.038

Curcumin nanoparticles containing poloxamer or soluplus tailored by high pressure homogenization using antisolvent crystallization

Alireza Homayouni[a*], Marjan Amini[a], Masoumeh Sohrabi[a], Jaleh Varshosaz[a], Ali Nokhodchi[b*],
[a]Department of Pharmaceutics, School of Pharmacy and Novel Drug Delivery Systems Research Center, Isfahan University of Medical Sciences, Isfahan, Iran;[b]Pharmaceutics Research Laboratory, Arundel Building, School of Life Sciences, University of Sussex, Brighton, BN1 9QJ, UK

*Corresponding authors: (Alireza Homayouni, a.r.homayouni@pharm.mui.ac.ir)

Ali Nokhodchi (a.nokhodchi@sussex.ac.uk)

Abstract

Curcumin is a natural active constituent of *Curcuma longa* from Zingiberaceae family that shows many different pharmacological effects such as anticancer, antioxidant, anti-inflammatory, antimicrobial and antiviral effect. However, its bioavailability is profoundly limited by its poor water solubility. In this study antisolvent crystallization followed by freeze drying was used for the preparation of curcumin nanoparticles. The presence of different ratios of hydrophilic polymers (poloxamer 188 & soluplus) on physicochemical properties of curcumin nanoparticles was also investigated. In addition, the effect of high pressure homogenization (HPH) on solubility and dissolution properties of curcumin was investigated. All nanoparticle formulations were examined to determine their particle size distribution, saturation solubility, morphology (SEM), solid state (DSC, XRPD and FT-IR) and dissolution behavior. It was observed that curcumin crystallized in the presence of polymers exhibited better solubility and dissolution rate in comparison with original curcumin. The results showed that the concentration of the stabilizer and the method used to prepare nanoparticles can control the dissolution of curcumin. The crystallized nanoparticles showed polymorph 2 curcumin with lower crystallinity and higher dissolution rate. Curcumin nanoparticles containing 50% soluplus prepared via HPH method presented 16-fold higher solubility than its original form. In conclusion, samples crystalized and proceed with HPH technique showed smaller particle size, better re-dispersibility, higher solubility and dissolution rate in water compared with a sample prepared using a simple antisolvent crystallization process.

Key words: curcumin, antisolvent crystallization, dissolution rate, high pressure homogenization

1. Introduction:

Curcumin, a polyphenol, is a yellow-orange pigment extracted from the powdered rhizomes of turmeric. Curcuminoids are only a small fraction of the turmeric rhizome and Curcumin compromises approximately 77% of the curcuminoid content. It is assumed that the major components of the commercial products are 77% curcumin, 17% dimethoxycurcumin and 3% bisdemethoxycurcumin with variances. It has been shown that Curcumin has a wide range of activities such as antioxidant, anti-inflammatory, antimicrobial, and anticarcinogenic activities (Goel et al., 2008).

Despite these medicinal benefits, curcumin shows a low oral bioavailability due to its poor aqueous solubility (11ng/ml at pH 5.0) and dissolution properties which greatly restricted its therapeutic use (Mohanty and Sahoo, 2010; Sanphui et al., 2011). Several strategies have been used to overcome this problem such as preparation of solid dispersion formulations (Li et al., 2015; Seo et al., 2012), use of polymeric nanoparticles (Beloqui et al., 2014; Fares and Salem, 2015), solid lipid nanoparticles (Kakkar et al., 2013; Sou et al., 2008), the use of micelles (Abouzeid et al., 2014; Song et al., 2014) and cyclodextrins (Tønnesen et al., 2002).

Among these methods reduction of particles to nanometer range could enhance both solubility and dissolution rate due to changes in the particle behavior proved by the Ostwald–Freundlich equation (Kesisoglou et al., 2007). There are two main techniques to manufacture nanoparticles (a) top-down and (b) bottom-up methods. In top-down techniques basilically equipment such as mill and high pressure homogenization (HPH) are used to reduced the size of particles (Shegokar and Müller, 2010; Van Eerdenbrugh et al., 2008), whereas in bottom-up techniques, nanoparticles can be obtained by molecular arrangement process such as precipitation or crystallization to control the size of nanoparticles (Sinha et al., 2013). Although, there are many techniques in bottom-up method to make nanoparticles, percipitation by the addition of non-solvent has been the most favorable method. In this system simply the drug is

dissolved in an organic solvent followed by the addition of an antisolvent (which is miscible with the solvent used to dissolve the drug) to precipitate the drug. One of the main problems with this technique is the crystal growth of particles after the precipitation. To overcome the crystal growth, generally, a stabilizer is added to the crystallization medium. The presence of the stablizer also inhibits the aggregation of nanoparticles. Furthermore, the case of using a hydrophilic stabilizer the wettability of hydrophobic drugs increased and this inturn can improve the solubility and oral bioavailability (Sinha et al., 2013; Thorat and Dalvi, 2012). This process is very popular as apart from improving the dissolution rate it can improve other pharmaceutical physicomechanical properties such as flowability and compressibility (Nokhodchi et al., 2015). On the basis of this, Baxter pharmaceutical company has invented a combination technology called 'NANOEDGE". In this method precipitated nanoparticles are subjected to high pressure homogenizer in order to inhibit the crystal growth and break down the large agglomerates (Rabinow, 2004). In addition to these attempts, the conditions of crystallization environment e.g. type of solvent, the ratio of solvent to antisolvent, the agitation of mixing etc. could affect the physicochemical properties of precipitates (Thorat and Dalvi, 2012).

In recent years many studies have been carried out to produce nanoparticles of curcumin by antisolvent crystallization, however, to the best of our knowledge, there is no specific study on the effect of soluplus and poloxamer as a stabilizer in nanoparticles of curcumin. In other words, the aim of this study is to investigate the effect of different ratios of soluplus and poloxamer on curcumin nanoparticles prepared by antisolvent crystallization. Moreover, in this study, the effect of high pressure homogenization on obtained nanosuspensions has been investigated. Although there are a few studies investigated the effect of antisolvent crystallization, HPH and freeze-drying, in each study only one method was used under different conditions and it is very difficult to justify the results obtained when comparing different methods published in different studies. There is no systematic and comprehensive study to investigated antisolvent, high pressure homogenization and freeze-drying together in a single study. Therefore, in the current study all three methods (antisolvent, HPH and freeze-drying) were employed on curcumin in a single study and the results can be elaborated better compared to previous study to enhance the dissolution rate of curcumin.

2. Materials and methods

2.1. Materials

Curcumin (Mitushi Biopharma, India), poloxamer 188 (Sigma, Germany), soluplus (BASF, Germany), and sodium dodecyl sulfate (Merck, Germany) were obtained. All other solvents and chemicals were of analytical grade.

2.2. Methods

2.2.1. Preparation of CUR:SOL and CUR:POL freeze dried nanoparticles precipitated by antisolvent crystallization method (CRS-FD)

Twenty milliliters of acetone was used to dissolve 1 g Curcumin. Various amounts of SOL or POL188 (0, 0.05, 0.1, 0.25 and 0.5 g) was separately dissolved in beakers containing 200 ml distilled water. The acetone solution containing curcumin was added dropwise (at a rate of 5 ml/min) using a burette into the aqueous solution with varying concentrations of the polymers stirring at 600 rpm at 25 °C to achieve various ratios of Curcumin:polymer (1:0, 20:1, 10:1, 4:1 or 2:1). The final suspension was immediately freezed at −70 °C followed by freeze drying (Martin Christ freeze dryer, Germany) for 48 h. Each crystallization experiment was performed in triplicate.

2.2.2. Preparation of CUR:SOL and CUR:POL freeze dried nanoparticles precipitated by antisolvent crystallization method followed by high pressure homogenizer (HPH-FD)

A FBF laboratory high pressure homogenizer (Italy) was used to process further the suspensions obtained from the antisolvent crystallization (CRS) process. The applied pressure was set at 500 and 1000 bars for 5 and 10 cycles respectively. The final suspension obtained after applying HPH was immediately freeze dried at −70 °C for 48 h. Each experiment was performed at least three times. The protocol used in the current research was based on the previously published articles elsewhere (Homayouni et al., 2014a;2014b).

2.2.3. Preparation of physical mixtures of drug carrier (PM)

In order to have a better comparison between the processed formulation and unprocessed formulations, physical mixtures of CUR and stabilizers were prepared as counterpart (the same ratios as the treated formulations were used) To this end, CUR, SOL or POL were sieved to get particle size fractions of less than 250 µm followed by mixing of CUR with SOL or POL using mortar and pestle for 2 min. The 2 min was good enough to get a good uniformity. The formulations were kept in well-tight containers until further use.

2.2.4. Morphological analysis

The morphology of nanosuspensions was examined using an optical microscope (OM) (Olympus BX-60, Japan) before freeze drying. In addition to the optical microscope, SEM images of the freeze dried particles were obtained using a scanning electron microscope (Philips X series, Netherlands) with an acceleration voltage of20 kV.

2.2.5. Particle size measurement

A nano-zetasizer (Malvern, UK) was employed for the measurement of the particle size of precipitates obtained via both CRS and HPH techniques. To do this end, deionized water was used the obtained nanosuspensions to get the concentration around 1 mg/ml. The measurements were carried out in triplicate and their mean and standard deviation of Z-average size and zeta potential of the particles were calculated.

2.2.6. Determination of saturation solubility

The saturation solubility of pure CUR, physical mixtures of CUR:SOL/POL and freeze dried samples obtained via different methods were determined according to the method published elsewhere (30). Briefly, around 2mg CUR was dispersed in 10 ml double-distilled

water in a beaker followed by agitation at 200 rpm at 25 °C for 48 h. The suspensions were then filtered through a 0.22 µm filter (MS® Nylon Syringe Filter) and then the concentration of the filtered suspension was measured at 426 nm (Shimadzu, Japan).

2.2.7. Differential scanning calorimetry (DSC)

DSC traces of the formulations was carried out using DSC 822e (Mettler Toledo, Switzerland) equipped with a refrigerated cooling system. Few of the samples which were vital in the current research were selected to determine their thermal behavior. In brief, few mg of the samples (2-3 mg) were placed in aluminum pans and sealed with a lid. The DSC pan containing the sample was scanned at a rate of 10 °C/min between 20 and 200 °C. The experiment was run under nitrogen gas at a flow rate of 80 ml/min. The thermal behaviors of the samples such as onset temperatures, melting points and endothermic and exothermic enthalpies were determined using the software provided (STARe Ver. 12.00 Mettler Toledo, Switzerland).

2.2.8. X-ray powder diffraction studies (XRPD)

The crystal state of the formulations was analyzed using XRPD. Scanning were carried out on selected samples using a D8 Advance diffractometer (Bruker, Germany) with Cu Kα radiation (λ = 1.54 Å) with scanning range of 5–80° (2Θ) with a step size of 0.05.

2.2.9. Fourier transform infrared spectroscopy (FT-IR)

As Curcumin may go under molecular changes during the crystallization, FT-IR (WQF-510/520 FTIR spectrophotometer, China) was used to study the changes in the molecular level of CUR in the formulations obtained.

Samples were prepared by potassium bromide (KBr) at a ratio of 1:10 and scanned against a blank KBr disk ranging from 4000 to 450 cm^{-1} with resolution of 1.0 cm^{-1}.

2.2.10. Dissolution studies

The dissolution behavior of curcumin formulations were examined using a USP dissolution apparatus, 2, paddle method (Pharmatest, Germany). The amount of dissolution medium (distilled water containing 0.25%w/v sodium dodecyl sulfate) in each vessel was 1000 ml which equilibrated to 37 °C with the paddle rotation of 50 rpm. Curcumin formulations equivalent to 10 mg CUR was placed at the top of the dissolution medium. At different time intervals, 5 ml of the dissolution medium was withdrawn and replaced by 5 ml fresh dissolution medium. The withdrawn solution was immediately filtered through 0.22 µm cellulose ester filter (MS® Nylon Syringe Filter) followed by reading the absorbance of the solution at a wavelength of 426 nm by spectrophotometer (Shimadzu, Japan). The concentration of the solution was then calculated on the basis of a calibration curve obtained for CUR at this wavelength. The dissolution was repeated 3 times for each formulation.

2.2.11. Dissolution parameters

For a better understanding and comparison on dissolution profiles, the dissolution efficiency (DE) and mean dissolution time (MDT) were determined using the following equations. In equation 1, DE represents the area under the dissolution curve (y) up to a certain time t, expressed as a percentage of the area of the rectangle described by 100% dissolution in the same time.

$$DE\% = \frac{\int_0^t y.dt}{y_{100}.t} \times 100 \quad \text{Equation 1}$$

Equation 2 represents MDT and it reflects the mean time of dissolution. In equation 2 $\bar{t}_i$ define the midpoint of the time period during which the fraction ΔM of the drug has been released from sample.

$$MDT = \sum \bar{t}_i .\Delta M_i / \sum \Delta M_i \qquad \bar{t}_i = (t_i + t_{i+1}) / 2 \qquad \Delta M_i = \left(M_{i+1} - M_i\right)$$

Equation 2

2.2.12. Re-dispersibility in water

In this test simply the powder was put on the surface of distilled water in a beaker and the re-dispersion of samples recorded photographically after 3 seconds.

Although the dissolution studies provide suitable results and indirectly shows how fast the particles could be dispersed and being wet in water, however this test has been done to illustrate visually and supports the dissolution results.

2.2.13. Statistical analysis

Statistical analysis was performed by one way analysis of variance (ANOVA) using Graph Pad Prism software (version 6.07). For all of the tests, the differences were considered as statistically significant where $P < 0.05$.

3. Results and discussion

Antisolvent crystallization is a simple and effective method to produce micro/nanoparticle of poorly water soluble drugs in order to improve its dissolution rate. In this study acetone and water have been used as a solvent and antisolvent for curcumin respectively. Among different solvents which can dissolve curcumin, acetone known as the best one because of high solubility and stability of curcumin in it and in addition this solvent could be evaporated as well at low temperature. Distilled water used as antisolvent because of its safety and cost-effectivness. In this study Soluplus and poloxamer 188 were used as stabilizer in order to inhibit crystal growth of curcumin. Moreover these carriers could accelerate wettability of curcumin simply because of their amphiphilic structures.

In section 2.2.2, the main reason to employ 5 cycles with 500 bars pressure was to pretreat suspension and it is important to use low pressure in HPH method to mill and breakdown the particles to achieve smaller particles. In addition, higher pressure at the first step could lead to aggregation of particles and blockage of the orifice of high pressure homogenizer.

3.1. Morphological analysis

Morphological analysis was performed in order to investigate the effect of crystallization techniques on the morphology of curcumin. Therefore, OM was used to investigate as an online scanning procedure. In this study, the effect of different ratios of stabilizers and also the effect of high pressure homogenization on morphology of particles after crystallization were investigated. In addition, scanning electron microscopy could illustrate the crystal habit of particles after freeze drying.

As shown in Fig. 1A. Freshly crystallized CUR without any stabilizer exhibited large aggregated particles while samples crystalized with different ratios of stabilizers (SOL or POL) showed very small and homogenous spherical particles (Fig. 1B with 5% soluplus).

To explore the effect of high pressure homogenization on the morphology of particles containing CUR, high pressure homogenizer was employed to produce nanosuspension with smaller particle size. Interestingly the sample subjected to the HPH produced larger particles with different morphologies. Figure 1C shows that HPH technique could break down the obtained spherical particles during homogenization. The formation of spherical particles in CRS samples could be attributted to the creation of temporary nanoemulsion droplets *(quasi-emulsion)* followed by the precipitation of the nanocrystals inside the droplets as a result of the counter-diffusion of the good solvent (acetone) and poor solvent (water) out and into the emulsion droplets respectively (Pignatello et al., 2002a; Pignatello

et al., 2002b; Pignatello et al., 2006). Similar results have obtained with antisolvent crystallization of celecoxib and PVP in our previous study (Homayouni et al., 2014c).

It can be concluded that the HPH method could change the morphology of CUR-CRS samples (Fig. 1C). During the homogenization, spherical temporary nanoparticles could be broken down by cavitation mechanism and this process could change the morphology of nanoparticles. As described before the nanospheres obtained with *QESD* (Quasi-emulsion solvent diffusion) method are unstable and could be destroyed by an aggressive procedure like HPH. This condition could be occurred also when these nanosuspensions were freeze dried. The freeze-dried samples were shown in Fig 2. CUR:SOL5% CRS-FD samples exhibited plate-shape particles as shown in Fig. 2B. These particles change to particles with similar –crystal habit after HPH process followed by freeze-drying (HPH-FD samples). However, it seems CUR:SOL5% HPH-FD presented lower mean particle size (Fig 2C). Similar results have been obtained with CUR:POL5% CRS-FD samples. In these samples, rod-shaped particles have been obtained (Fig 2D) whereas those formulations manufcatured uisng antisolvent crystallization and HPH followed by freeze drying (HPH-FD) exhibited smaller particles with platy morphology (Fig 2E). Different crystal habits was also reported elsewhere (Thorate and Dalvi, 2015) where CUR could crystallize in three polymorphic forms. Form 1 (monoclinic structure) whereas Forms 2 and 3 exist as orthorhombic structures. Liquid antisolvent crystallization of CUR with additive and/or ultrasound resulted orthorhombic forms (Form 2 or Form 3) with different crystal habits (depending on each additive used) while crystallization of CUR without any additive or ultrasound produce monoclinic form with star-like crystal. In another study Yadav and Kumar (2014) prepared nanoparticle of CUR by antisolvent crystallization. The freshly crystallized CUR with and without any additive showed spherical nanoparticles however these nanoparticles converted to star-like crystal after 1.5 hour and after 3 hours these crystals aggregate together to form platy-shape crystals. While the spherical nanoparticle obtained with 0.5% Gelatin (as stabilizer) could retain its shape after 3 hours (Yadav and Kumar, 2014).

3.2. Particle size measurement

Particle size measurement was performed to investigate the effect of different stabilizers and also various ratios of them on the mean particle size of the formulations. Moreover, the effect of processing method (HPH and freeze drying) has been studied for this section.

The results in Table 1 showed that the particles obtained through the antisolvent crystallization technique (CRS) showed smaller particle size compared to the HPH technique. Statistical analysis showed this difference is significant ($p < 0.05$). Moreover, in general, the PDI of these samples become higher after HPH process. As described in optical microscopy section, when CRS samples subjected to high pressure homogenizer, the unstable nanoemulsion droplets of CUR/stabilizer could be brokenen down during HPH process and then an increase in the size of particles obtained.

Comparing of freeze dried samples (CRS-FD and HPH-FD) with non-freeze dried samples (CRS and HPH) showed that the mean particle size of these samples become greater ($p < 0.05$) that could be predictable. By freezing the water and sublimation of ice, the freely mobilize particles in suspension could aggregate together; hence re-dispersion of these particles could not simply happen after freeze drying so generally the mean particle size of freeze dried samples is greater than non-freeze dried samples.

The interesting result in Table 1 is the comparison of mean particle size of HPH-FD samples with CRS-FD ones. As described before the mean particle size of samples obtained via CRS was smaller than the samples obtained via HPH method, while in freeze dried samples the mean particle size of HPH-FD was smaller than CRS-FD samples. Moreover, generally the PDI of HPH-FD samples are smaller than PDI of CRS-FD samples. This result shows the ability of HPH process to generate particles with more dispersability after freeze drying. The CRS samples showed smaller particle size than samples produced by HPH method (without any freeze drying). However these small particles in both CRS and HPH methods are not stable enough and could be disturbed and aggregated if they were subjected to any aggressive conditions such as freeze-drying. When the both samples (CRS and HPH) were freeze-dried it seems the particles produced by CRS have more tendency to aggregate due to having smaller particle size and larger surface area compared to HPH samples. Therefore, the aggregation in CRS samples should be much higher and stronger than HPH samples (due to differences in their particle size). When the particle size is measured for freeze-dried samples the force applied to deaggregate the particles is not good enough, therefore, samples obtained via CRS-FD should be larger than the samples obtained via HPH-FD. This

indicates that larger particles of curcumin is less influenced by freeze-drying process compared to smaller curcumin particles which could be an advantage for HPH method used in the current research. This was also supported by the fact that high pressure homogenizer (HPH method) could produce nanocrystals with narrow PDI with a suitable re-dispersibility (Keck and Muller, 2006.)

Comparing of the mean particle size of the samples prepared with SOL or POL showd no remarkable results nor for different ratios of carriers.

3.3. Determination of saturation solubility

The saturation solubility analysis was performed on pure CUR, physical mixtures (PM), CRS-FD and HPH-FD samples. The solubility study of raw CUR showed very low solubility in distilled water (0.18 µg/ml), although the solubility has been improved in crystallized and homogenized pure CUR, however this enhancement was not significant ($p > 0.05$). As shown in Fig. 3 the presence of stabilizers increased the solubility of CUR in PM, CRS-FD and HPH-FD samples. This enhancement in the solubility became greater by increasing the stabilizer contribution in the formulations that could be attributed to the solubilizing effect of SOL and POL as the amphiphilic polymers. SOL and POL could generate micelles in water and dissolve the CUR molecules. These stabilizers with hydrophilic groups along with the lipophilic chain are able to interact with hydrophobic drugs and finally accelerate the hydration of poorly-water soluble drugs (Homayouni et al., 2014a; Homayouni et al., 2015). Comparison of solubility data -among PMs and crystallized samples (CRS-FD and HPH-FD) demonstrated that HPH-FD formulations in the presence of SOL or POL have been more effective in enhancing the solubility of CUR than PM and CRS-FD samples. Statistical analysis showed that all HPH-FD samples showed higher saturation solubility compare to PM and CRS-FD samples ($p < 0.05$). for instance, the saturation solubility of CUR in CUR:SOL 50% HPH-FD sample was 2.96 µg/ml while this amount was 0.59 µg/ml and 0.49 µg/ml for CRS-FD and PM samples respectively. Although the CRS-FD samples showed higher solubility compared to its physical mixtures, however, high pressure homogenization followed by antisolvent crystallization could be more effective than simple antisolvent crystallization technique. It

seems the method of preparation plays a critical role on saturation solubility of CUR in these samples. The higher solubility of HPH-FD samples compared to other samples could be due to the smaller mean particle size of these samples. According to Table 1, generally, HPH-FD samples in the presence of SOL or POL in different ratios showed smaller particles size with narrower PDI.

3.4. Differential scanning calorimetry (DSC)

In order to investigate any interaction between drug and stabilizers, DSC analysis has been performed. In addition, any changes in the polymorphic form of CUR and also in the generation of amorphous state of CUR during crystallization process could be detected through this thermal analysis. Fig 4 shows the DSC traces of untreated CUR, physical mixture samples with 50%SOL and 50%POL and also crystallized samples with the same ratios. The untreated CUR exhibited an endothermic peak near 176 °C corresponding to its melting point which reported previously in literature data (Donsì et al., 2010; Kakran et al., 2012; Sanphui et al., 2011). CUR samples crystallized in the absence of any stabilizers (CUR CRS-FD) exhibited a different pattern in its thermogram. This sample showed two endothermic peaks near 162 °C and 157 °C. Comparison of DSC traces of untreated CUR and CUR CRS-FD sample indicated the presence of new polymorph during the crystallization process. Moreover, the enthalpy of fusion reduced from 82 J/g for untreated CUR to 74 J/g for CUR CRS-FD sample. This reduction confirmed the reduced crystallinity of curcumin during the crystallization process. Previous studies have also reported the possibility of the presence of different polymorphic forms of curcumin during crystallization (Sanphui et al., 2011; Thorat and Dalvi, 2014; Thorat and Dalvi, 2015). Kakran and Sahoo (2012) prepared CUR by antislovent crystallization with ethanol and water as solvent and antisolvent respectively however the DSC trace of crystallized CUR were similar to raw CUR (Kakran and Sahoo, 2012). As describe before it seems the condition of crystallization could affect the solid state of crystalized CUR.

CUR:SOL 50% PM sample showed the melting endothermic peak of curcumin near 176 °C, however the intensity of peak reduced and broadened. In CUR:POL 50% PM a large endothermic peak appeared near 55 °C corresponded to the melting point of poloxamer 188. The absence of CUR melting endothermic peak in this sample is attributed to the dissolution of CUR in the molten POL. In

CUR:POL 50% CRS-FD sample similar result was obtained. Reduction in the melting point of POL to 55 °C could be attributed to the penetration of CUR molecules into the crystalline structure of POL during crystallization. As a result, POL present lower crystalline structure, compared to its primary form. Therefore, it could be melted at a lower temperature with broad melting peak. A similar condition could occur for CUR. Reduction in CUR melting point to lower temperature with broader peak and lower intensity exhibited the formation of a matrix between CUR and POL. In the crystallized sample prepared with 50% SOL similar result was obtained. In CUR:SOL50% CRS-FD the peak intensity of CUR melting point was reduced to 166 °C with an enthalpy of fusion 16 J/g compared to its physical mixtures with 33 J/g value. This result indicates that most part of CUR present in amorphous nature in this sample. Similar results have been reported for celecoxib with solplus and poloxamer (Homayouni et al., 2014a; Homayouni et al., 2014b).

3.5. X-ray powder diffraction studies (XRPD)

The results of XRPD studies are depicted in Fig.5. X-ray diffraction of CUR showed sharp peaks at 2Θ values of 9.15°, 10.3°, 14.2°, 16.9°, 20.1° and 21.1° which is an indication of crystalline state of curcumin. As shown in Fig 5, CUR-CRS sample showed similar pattern to CUR but with smaller intensity that could be due to the lower crystallinity of the treated sample. Moreover, in CUR CRS-FD sample, the presence of a new peak at 16.2° demonstrated the existence of a new polymorphic form of curcumin in this sample. Previous studies have been reported the probability of curcumin polymorph formation during crystallization (Sadeghi et al., 2016; Thorat and Dalvi, 2014; Thorat and Dalvi, 2015). It seems CUR CRS-FD sample contains both amorphous and polymorphic forms of curcumin. Comparison the XRPD pattern of the samples obtained via CRS-FD and HPH-FD did not show any significant difference which proved that the HPH process did not change the solid state of curcumin. Although, a reduction in the peak intensity of CUR-SOL50% HPH-FD and CUR-POL50% HPH-FD could be an indication of a reduction in crystallinity of curcumin in these samples, the presence of a new peak at 16.2° indicating the mixture of amorphous and polymorphic form in the sample. The PXRD result also supported the DSC findings for the crystallized samples.

3.6. Fourier transform infrared spectroscopy (FT-IR)

FT-IR was also used to study the molecular interactions between the CUR and the stabilizers. Moreover, FT-IR study could exhibit the amorphous nature and the presence of any polymorphism of curcumine. The FT-IR spectrums of untreated curcumin, CUR-CRS and crystalized samples prepared with 50% stabilizer were showed in Fig 6. Untreated curcumin showed a characteristic peak at 1628 cm^{-1} corresponded to its carbonyl group participate in intramolecular hydrogen bonding. It has been demonstrated that curcumin exhibits keto-enol tautomerism. Single crystallography analyses have shown that the most favorable form of curcumin is the keto-enol form (Sanphui et al., 2011). Resonance-assisted intramolecular hydrogen bond stabilized this conformation. Formation of an intramolecular hydrogen bond leads to change of wave number of the carbonyl stretching band from 1700 cm^{-1} to 1628 cm^{-1}. The CUR-CRS sample showed the same band at 1628 cm^{-1} indicating that the intramolecular hydrogen bonded keto-enol tautomer exists in this sample too. Moreover it has been reported before that crystalline curcumin (form 1) participate in intramolecular hydrogen bonds between the phenolic groups and methoxy substituents, oriented ortho to one another on the phenyl ring (Wegiel et al., 2014). With these conditions possibility of hydrogen bonding between curcumin and a polymer will be weak. As reported in literatures, untreated curcumin (form 1) showed characteristic peaks at 1628 cm^{-1} attributed to carbonyl group (described above), at 1601 cm^{-1} belong to aromatic C=C stretching, at 1429 cm^{-1} due to phenolic C-O stretching, at 1281 cm^{-1} due to enolic C-O stretching and a sharp peak at 3508 cm^{-1} which is attributed to OH stretching (Sanphui et al., 2011). These wavenumbers for crystalline curcumin (form 1) is compatible with our untreated CUR as shown in Fig 6, but in CUR-CRS sample some of these peaks have been shifted. The OH stretching bond has been changed from 3508 cm^{-1} to 3406 cm^{-1} and 3259 cm^{-1}. Moreover, the C=C aromatic stretching at 1601 cm^{-1} bifurcated to 1601 cm^{-1} and 1587 cm^{-1}. In addition, the phenolic C-O stretching at 1281 cm^{-1} bifurcated also to and 1281 cm^{-1} and 1263 cm^{-1} (Fig 6B). All these changes demonstrated the formation of new polymorph during crystallization. Sanphui *et al* reported these changes previously in FT-IR spectrum that could be due to the presence of polymorph 2 in curcumin. They are also reported that in form 2, curcumin is less crystalline compared to form 1 or the content of amorphous in form 2 is higher than other polymorphs

(Sanphui et al., 2011). In conclusion, all the above descriptions proved that CUR-CRS sample contains polymourph 2. These results supported the DSC and XRPD findings.

As described above it might be projected that curcumin hydrogen bonding with a stabilizer could occur between phenolic OH group of curcumin and an electronegative group of a carrier. As shown in Fig 6 SOL showed large and broad spectrum at 1643 cm^{-1} and 1739 cm^{-1} corresponding to tertiary amide and ester carbonyl stretching respectively. However, according to a large number of C=O group of SOL compared to OH groups of CUR it could not simply show the formation of hydrogen bonding with FT-IR spectrum. In other words, in case of hydrogen bonding, the number of non-bonded C=O groups are more than carbonyl group which participate in hydrogen bonding. Therefore this results leads to a negligible shift in the C=O stretching vibration band. The changes in OH groups position of curcumin and broadening the peaks might be due to the presence of curcumin in amorphous nature (Sanphui et al., 2011) or formation of hydrogen bond between curcumin and soluplus. FT-IR spectrum of poloxamer 188 and curcumin did not add useful results.

3.7. Dissolution studies

The dissolution pattern of original CUR and treated samples are shown in Fig. 7. For comparison purpose the dissolution profile of physical mixtures of curcumin and polymers (PM) were plotted and shown in Figures 7A and B. The results showed that the presence of POL or SOL enhanced the disolution rate of curcumin and this enhancement become more apparent when the concentration of the stabilizers increased (Fig. 7A and B). The increase in the dissolution is due to hydrophilic nature and surfactant properties of the stabilizers which could accelerate the hydration of lipophilic drugs as discussed before in the saturation solubility section. It can be concluded that the presence of POL or SOL is useful to improve the dissolution rate of curcumin. It was interesting to note that the dissolution rate of curcumin can be further increased by treating the samples via crystallizations or HPH methods (Figs. 7C, D, E and F). The reason for the further enhancement in the dissolution could be due to the smaller particle size in these samples compared to their PM counterpart. Moreover, in these samples during crystallization process, stabilizer (POL or SOL) could attach to the surface of

curcumin particles during crystal growth and inhibit the aggregation of nanoparticles. As shown in Figs. 7C and D the dissolution enhancement become accelerated by increasing the polymer ratios. It is obvious that increasing the polymer ratio could accelerate the dissolution rate of CUR because of the surfactant properties of the polymers (both POL and SOL). Moreover these carriers could act as stabilizer so the higher ratios of polymers could be more effective to inhibit the crystal growth of CUR particles during the crystallization process. These results can be backed up by few references (Homayouni et al., 2014b; Homayouni et al., 2014c; Sinha et al., 2013; Thorat and Dalvi, 2012). Comparing the dissolution profiles of samples obtained via CRS for both POL and SOL showed that SOL formulations showed slightly faster dissolution compared to POL formulations. For instance, CUR:SOL50% CRS-FD showed about 80% dissolution after 40 minutes while this value was 62% for CUR:POL50% CRS-FD sample at the same time. The results also showed that, generally, samples obtained through HPH showed higher dissolution rate compared to the samples obtained through CRS method. The results of percentage dissolution efficiency (DE) and mean dissolution time (MDT) also demonstrated these findings (Table 2). In HPH-FD samples with higher concentration of polymer almost all of curcumin released after 40 min. for example in CUR:POL50% HPH-FD sample 98% of curcumin released after 40 min while this value is 68% after 40 min for CUR:POL50% CRS-FD sample. The reason for this phenomenon could be due to having the smaller particle size for HPH-FD samples compared to CRS-FD samples (Table 1 and Fig. 2). The results obtained from table 2 and figure 7, demonstrated the better performance of particles obtained through HPH-FD compared to CRS-FD samples particularly at lower concentration of stabilizer. These results are in line with the saturation solubility studies. Comparing the dissolution efficacy and dissolution profile data (reported in Table 2 and Fig 7) between CRS-FD and HPH-FD samples showed that at high concentration of polymer (50%), HPH process does not show impressive effect on DE% (table 2) while at low concentration of polymer (both POL and SOL) methods of manufacture and effect of HPH process, play a critical role on dissolution enhancement of curcumin. In the other word at high concentration ratio of stabilizer the dissolution rate depended on polymer ratio and HPH process could not show its effect as well as at low concentration ratios of stabilizer (5%, 10% and 25%). Several studies have been demonstrated the high efficiency of HPH process for enhancing the dissolution rate of several drugs (Donsì et al., 2010; Keck and Muller, 2006; Shegokar and Müller, 2010).

The dissolution profile of CUR-CRS-FD and CUR-HPH-FD samples did not show any remarkable change compared to untreated CUR, although a small enhancement could be seen similar to saturation solubility results.

3.8. Re-dispersibility in water

Amount of re-dispersibility of lipophilic drugs in water shows the accurate predictions of solubility and dissolution as the first step of absorption in gastrointestinal tract. In this test re-dispersion of samples recorded by camera after the powder was placed on the surface of distilled water in a beaker. As shown in fig 8A the CUR CRS-FD did not re-dispersed in water like untreated CUR due to its high lipophilic nature however CUR-HPH-FD sample re-dispersed easily and became wet better than other samples. Fig 8B and C showed the HPH samples prepared with 25% POL and 25% SOL re-dispersed in water easily. The orange color of water illustrated this phenomenon as well. This test as visual study resulted the ability of HPH samples to be dispersed and wet in water. These results are in good agreement with saturation solubility and dissolution studies. The obtained results can be supported by the research work carried out by Donsi *et al* (2010). In previous study CUR sub-micron dispersions have been prepared by high pressure homogenization of pure CUR. The resulted CUR shows better water dispersity compare to untreated CUR. The mechanism has been expressed behind this results was reduction of CUR particle size and reduction of crystallinity caused by mechanical stress (Donsi et al., 2010). It seems in this study we have the same condition moreover the presence of stabilizers (hydrophilic polymers) could enhance re-dispersibility of CUR by surfactant properties.

4. Conclusion

It was shown that antisolvent crystallization of curcumin with acetone and water as solvent and antisolvent produced curcumin polymorph with different physicochemical properties. Soluplus and poloxamer 188 are potential stabilizers to be used in antisolvent crystallization followed by high pressure homogenization to produce nanoparticles with higher dissolution velocity. High pressure homogenization could be more effective than others in producing very fine particle size of curcumin nanoparticles and as a result more

effective in enhancing the solubility and dissolution of curcumin. Sample crystalized and homogenized with 50% soluplus (CUR:SOL50% HPH-FD) exhibited about 16-fold higher solubility compare to untreated curcumin.

Acknowledgments

The authors thanked the Vice Chancellor Research of Isfahan University of Medical Sciences, Iran (Grant no. 395488) for the financial support. The author is gratefully appreciated to Pasaddak Company, for providing gift sample of Soluplus®

References

Abouzeid, A.H., Patel, N.R., Torchilin, V.P., 2014. Polyethylene glycol-phosphatidylethanolamine (PEG-PE)/vitamin E micelles for co-delivery of paclitaxel and curcumin to overcome multi-drug resistance in ovarian cancer. International Journal of Pharmaceutics 464, 178-184.

Beloqui, A., Coco, R., Memvanga, P.B., Ucakar, B., des Rieux, A., Préat, V., 2014. pH-sensitive nanoparticles for colonic delivery of curcumin in inflammatory bowel disease. International Journal of Pharmaceutics 473, 203-212.

Donsì, F., Wang, Y., Li, J., Huang, Q., 2010. Preparation of Curcumin Sub-micrometer Dispersions by High-Pressure Homogenization. Journal of Agricultural and Food Chemistry 58, 2848-2853.

Fares, M.M., Salem, M.t.S., 2015. Dissolution enhancement of curcumin via curcumin–prebiotic inulin nanoparticles. Drug Development and Industrial Pharmacy 41, 1785-1792.

Goel, A., Kunnumakkara, A.B., Aggarwal, B.B., 2008. Curcumin as "Curecumin": From kitchen to clinic. Biochemical Pharmacology 75, 787-809.

Homayouni, A., Sadeghi, F., Nokhodchi, A., Varshosaz, J., Garekani, H.A., 2014a. Preparation and characterization of celecoxib solid dispersions; comparison of poloxamer-188 and PVP-K30 as carriers. Iranian Journal of Basic Medical Sciences 17, 322-331.

Homayouni, A., Sadeghi, F., Nokhodchi, A., Varshosaz, J., Garekani, H.A., 2015. Preparation and characterization of celecoxib dispersions in soluplus®: Comparison of spray drying and conventional methods. Iranian Journal of Pharmaceutical Research 14, 35-50.

Homayouni, A., Sadeghi, F., Varshosaz, J., Afrasiabi Garekani, H., Nokhodchi, A., 2014b. Promising dissolution enhancement effect of soluplus on crystallized celecoxib obtained through antisolvent precipitation and high pressure homogenization techniques. Colloids and Surfaces B: Biointerfaces 122, 591-600.

Homayouni, A., Sadeghi, F., Varshosaz, J., Garekani, H.A., Nokhodchi, A., 2014c. Comparing various techniques to produce micro/nanoparticles for enhancing the dissolution of celecoxib containing PVP. European Journal of Pharmaceutics and Biopharmaceutics 88, 261-274.

Kakkar, V., Mishra, A.K., Chuttani, K., Kaur, I.P., 2013. Proof of concept studies to confirm the delivery of curcumin loaded solid lipid nanoparticles (C-SLNs) to brain. International Journal of Pharmaceutics 448, 354-359.

Kakran, M., Sahoo, N., Tan, I.L., Li, L., 2012. Preparation of nanoparticles of poorly water-soluble antioxidant curcumin by antisolvent precipitation methods. J Nanopart Res 14, 1-11.

Keck, C.M., Muller, R.H., 2006. Drug nanocrystals of poorly soluble drugs produced by high pressure homogenisation. European journal of pharmaceutics and biopharmaceutics : official journal of Arbeitsgemeinschaft fur Pharmazeutische Verfahrenstechnik e.V 62, 3-16.

Kesisoglou, F., Panmai, S., Wu, Y., 2007. Nanosizing — Oral formulation development and biopharmaceutical evaluation. Advanced Drug Delivery Reviews 59, 631-644.

Li, J., Lee, I.W., Shin, G.H., Chen, X., Park, H.J., 2015. Curcumin-Eudragit® E PO solid dispersion: A simple and potent method to solve the problems of curcumin. European Journal of Pharmaceutics and Biopharmaceutics 94, 322-332.

Mohanty, C., Sahoo, S.K., 2010. The in vitro stability and in vivo pharmacokinetics of curcumin prepared as an aqueous nanoparticulate formulation. Biomaterials 31, 6597-6611.

Nokhodchi, A., Homayouni, A., Araya, R., Kaialy, W., Obeidat, W., Asare-Addo, K., 2015. Crystal engineering of ibuprofen using starch derivatives in crystallization medium to produce promising ibuprofen with improved pharmaceutical performance. RSC Advances 5, 46119-46131.

Pignatello, R., Bucolo, C., Ferrara, P., Maltese, A., Puleo, A., Puglisi, G., 2002a. Eudragit RS100® nanosuspensions for the ophthalmic controlled delivery of ibuprofen. European Journal of Pharmaceutical Sciences 16, 53-61.

Pignatello, R., Bucolo, C., Spedalieri, G., Maltese, A., Puglisi, G., 2002b. Flurbiprofen-loaded acrylate polymer nanosuspensions for ophthalmic application. Biomaterials 23, 3247-3255.

Pignatello, R., Ricupero, N., Bucolo, C., Maugeri, F., Maltese, A., Puglisi, G., 2006. Preparation and characterization of eudragit retard nanosuspensions for the ocular delivery of cloricromene. AAPS PharmSciTech 7, E27.

Rabinow, B.E., 2004. Nanosuspensions in drug delivery. Nature reviews. Drug discovery 3, 785-796.

Sadeghi, F., Ashofteh, M., Homayouni, A., Abbaspour, M., Nokhodchi, A., Garekani, H.A., 2016. Antisolvent precipitation technique: A very promising approach to crystallize curcumin in presence of polyvinyl pyrrolidon for solubility and dissolution enhancement. Colloids and Surfaces B: Biointerfaces 147, 258-264.

Sanphui, P., Goud, N.R., Khandavilli, U.B., Bhanoth, S., Nangia, A., 2011. New polymorphs of curcumin. Chem Commun (Camb) 47, 5013-5015.

Seo, S.-W., Han, H.-K., Chun, M.-K., Choi, H.-K., 2012. Preparation and pharmacokinetic evaluation of curcumin solid dispersion using Solutol® HS15 as a carrier. International Journal of Pharmaceutics 424, 18-25.

Shegokar, R., Müller, R.H., 2010. Nanocrystals: Industrially feasible multifunctional formulation technology for poorly soluble actives. International Journal of Pharmaceutics 399, 129-139.
Sinha, B., Müller, R.H., Möschwitzer, J.P., 2013. Bottom-up approaches for preparing drug nanocrystals: Formulations and factors affecting particle size. International Journal of Pharmaceutics 453, 126-141.
Song, Z., Zhu, W., Liu, N., Yang, F., Feng, R., 2014. Linolenic acid-modified PEG-PCL micelles for curcumin delivery. International Journal of Pharmaceutics 471, 312-321.
Sou, K., Inenaga, S., Takeoka, S., Tsuchida, E., 2008. Loading of curcumin into macrophages using lipid-based nanoparticles. International Journal of Pharmaceutics 352, 287-293.
Thorat, A.A., Dalvi, S.V., 2012. Liquid antisolvent precipitation and stabilization of nanoparticles of poorly water soluble drugs in aqueous suspensions: Recent developments and future perspective. Chemical Engineering Journal 181–182, 1-34.
Thorat, A.A., Dalvi, S.V., 2014. Particle formation pathways and polymorphism of curcumin induced by ultrasound and additives during liquid antisolvent precipitation. CrystEngComm 16, 11102-11114.
Thorat, A.A., Dalvi, S.V., 2015. Solid-State Phase Transformations and Storage Stability of Curcumin Polymorphs. Crystal Growth & Design 15, 1757-1770.
Tønnesen, H.H., Másson, M., Loftsson, T., 2002. Studies of curcumin and curcuminoids. XXVII. Cyclodextrin complexation: solubility, chemical and photochemical stability. International Journal of Pharmaceutics 244, 127-135.
Van Eerdenbrugh, B., Van den Mooter, G., Augustijns, P., 2008. Top-down production of drug nanocrystals: Nanosuspension stabilization, miniaturization and transformation into solid products. International Journal of Pharmaceutics 364, 64-75.
Wegiel, L.A., Zhao, Y., Mauer, L.J., Edgar, K.J., Taylor, L.S., 2014. Curcumin amorphous solid dispersions: the influence of intra and intermolecular bonding on physical stability. Pharmaceutical development and technology 19, 976-986.
Yadav, D., Kumar, N., 2014. Nanonization of curcumin by antisolvent precipitation: Process development, characterization, freeze drying and stability performance. International Journal of Pharmaceutics 477, 567-577.

Figures captions

Figure 1. Optical microscope image of (A) curcumin obtained from anti solvent crystallization (CUR-CRS), (B) curcumin obtained from anti solvent crystallization at presence of 5% soluplus, (C) curcumin obtained from anti solvent crystallization followed by high pressure homogenization at presence of 5% soluplus.

Figure 2. SEM image of (A) untreated curcumin, (B) CRS-FD samples with 5% soluplus, (C) HPH-FD samples with 5% soluplus, (D) CRS-FD samples with 5% poloxamer, (E) HPH-FD samples with 5% poloxamer.

Figure 3. Saturation solubility of untreated curcumin, samples prepared with physical mixture (PM), freeze dried samples prepared by antisolvent crystallization (CRS-FD) and freeze dried samples prepared by antisolvent crystallization followed by high pressure homogenization (HPH-FD).

Figure 4. DSC traces of pure CUR, physical mixture (PM), freeze dried samples prepared by antisolvent crystallization (CUR CRS-FD) and freeze dried samples prepared by antisolvent crystallization in the presence of 50% of soluplus or poloxamer.

Figure 5. XRPD pattern of untreated CUR, samples prepared by antisolvent crystallization (CRS-FD) and samples prepared by antisolvent crystallization followed by high pressure homogenization (HPH-FD) in the presence of 50% of soluplus or poloxamer.

Figure 6. FT-IR spectra of untreated CUR, samples obtained through antisolvent crystallization techniques (CRS) in the presence of 50% soluplus or poloxamer.

Figure 7. Dissolution profiles for different samples: (A, B) physical mixtures of CUR and stabilizers, (C,D) freeze dried samples prepared by antisolvent crystallization with stabilizers, (E,F) freeze dried samples prepared by antisolvent crystallization followed by high pressure homogenization of CUR and stabilizers (HPH-FD). (n = 3, and error bars are standard deviation).

Figure 8. Re-dispersibility of different samples in water. (A) without stabilizer, (B) with 25% poloxamer, (C) with 25% soluplus.

Table 1. Particle size of untreated CUR and CUR:SOL/POL samples prepared by different procedures

SAMPLE	z-average CRS (nm)	PdI	Zeta-potential	z-average HPH (nm)	PdI	z-average CRS-FD (nm)	PdI	z-average HPH-FD (nm)	PdI
CUR	ND	ND	-31	ND	ND	ND	ND	ND	ND
POL 5%	311 ± 82	0.425 ± 0.041	-30	701 ± 89	0.571 ± 0.121	1296 ± 601	0.712 ± 0.122	1021 ± 452	0.651 ± 0.089
POL 10%	259 ± 42	0.366 ± 0.052	-23	543 ± 54	0.459 ± 0.062	2399 ± 423	1	1333 ±369	0.538 ± 0.092
POL 25%	396 ± 35	0.463 ± 0.067	-29	475 ± 71	0.371 ± 0.059	1421 ± 398	0.491 ± 0.072	1399 ± 569	1
POL 50%	339 ± 57	0.293 ± 0.051	-19	616 ± 64	0.416 ± 0.081	1761 ± 405	0.727 ± 0.113	815 ± 402	0.662 ± 0.121
SOL 5%	258 ± 48	0.305 ± 0.059	-23	491 ±75	0.579 ± 0.066	2026 ± 367	1	1053 ± 825	0.526 ± 0.106
SOL 10%	218 ± 55	0.325 ± 0.046	-21	778 ± 109	0.601 ± 0.089	6515 ± 536	0.569 ± 0.141	1229 ± 768	0.216 ± 0.075
SOL 25%	220 ± 38	0.122 ± 0.039	-22	691 ± 97	0.524 ± 0.071	4493 ± 406	1	2739 ± 655	0.562 ± 0.096
SOL 50%	459 ± 185	0.552 ± 0.041	-12	891 ± 45	0.149 ± 0.052	4033 ± 569	0.469 ± 0.086	3371 ± 504	0.464 ± 0.108

Table 2. Dissolution efficiency (DE) and mean dissolution time (MDT) of untreated CUR and CUR:SOL/POL samples prepared with physical mixture (PM), antisolvent crystallization (CRS) and crystallization followed by high pressure homogenization (HPH).

Sample	Theoretical loading*	Actual loading *	DE40 %	MDT (min)	Sample	Theoretical loading	Actual loading	DE40 %	MDT (min)
CUR	100	100	7.81	19.38	**CUR**	100	100	7.81	19.38
CUR CRS-FD	100	100	10.93	16.16	**CUR CRS-FD**	100	100	10.93	16.16
CUR HPH-FD	100	100	14.34	15.44	**CUR HPH-FD**	100	100	14.34	15.44
POL 5% PM	100	100	9.27	13.85	**SOL 5% PM**	100	100	12.99	12.27
POL 10% PM	100	100	10.11	12.59	**SOL 10% PM**	100	100	10.66	19.01
POL 25% PM	100	100	14.28	15.80	**SOL 25% PM**	100	100	16.87	11.45
POL 50% PM	100	100	15.71	14.70	**SOL 50% PM**	100	100	18.99	14.30
POL 5% CRS-FD	95.2	95.3±1.2	16.71	14.12	**SOL 5% CRS-FD**	95.2	95.4±2.8	26.97	13.86
POL 10% CRS-FD	90.9	89.7±1.1	14.48	17.90	**SOL 10% CRS-FD**	90.9	90.6±3.1	37.18	13.27
POL 25% CRS-FD	80	79.1±0.5	41.49	10.54	**SOL 25% CRS-FD**	80	79.4±1.9	41.79	10.46
POL 50% CRS-FD	66.7	66.5±1.4	59.60	5.19	**SOL 50% CRS-FD**	66.7	65.9±1.2	64.47	7.42
POL 5% HPH-FD	95.2	91.7±1.5	36.22	13.02	**SOL 5% HPH-FD**	95.2	90.9±0.7	37.24	8.02
POL 10% HPH-FD	90.9	80.5±3.8	35.81	14.52	**SOL 10%**	90.9	83.4±2.7	41.09	8.19

					HPH-FD				
POL 25% HPH-FD	80	69.1±2.4	70.03	7.00	**SOL 25% HPH-FD**	80	74.1±3.5	62.37	10.69
POL 50% HPH-FD	66.7	65.6±3.1	70.50	10.55	**SOL 50% HPH-FD**	66.7	64.3±1.3	65.54	13.20

- As these are physical mixtures and the drug was added manually, therefore, the value of assay for all these physical mixtures should be 100%.

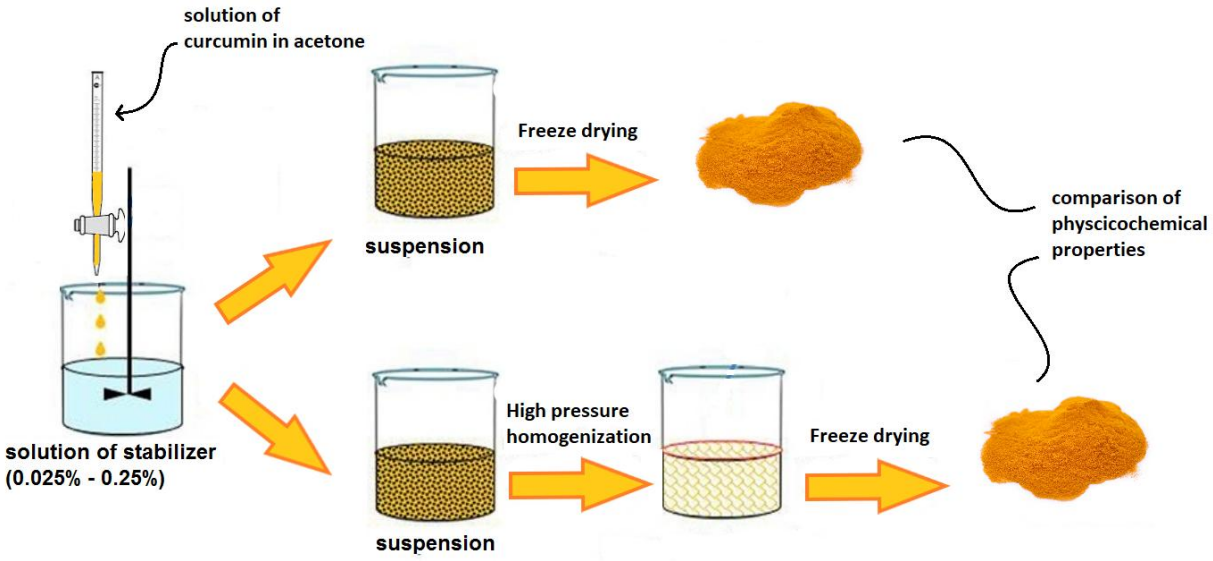

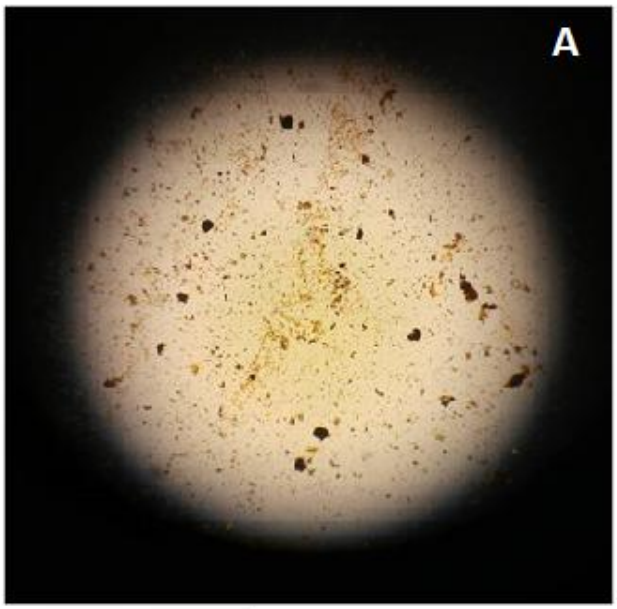
A

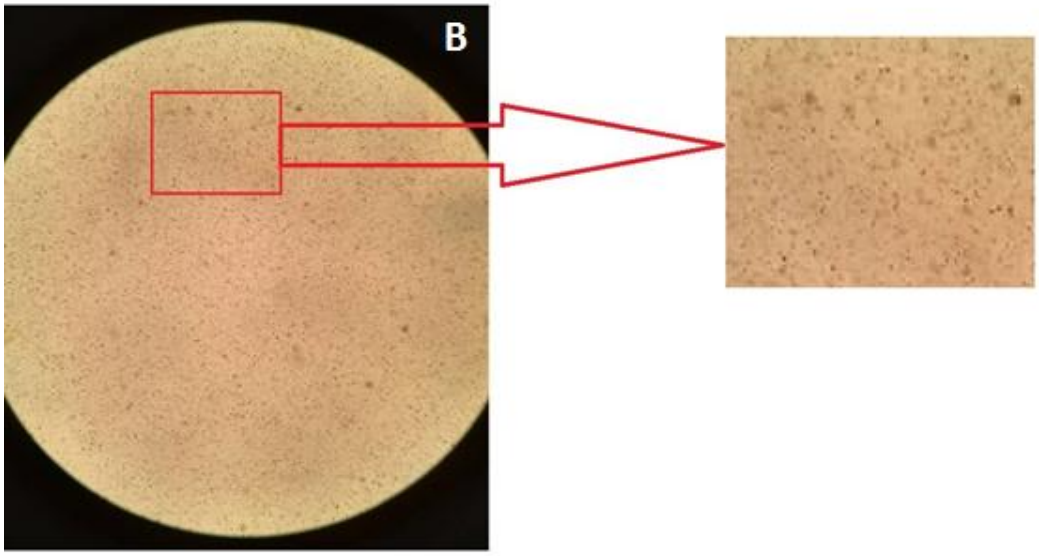
B

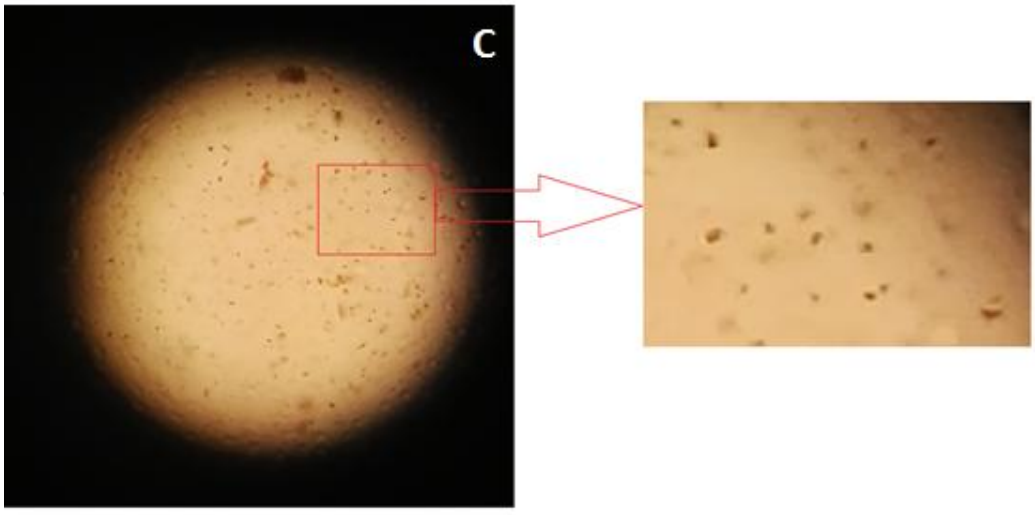
C

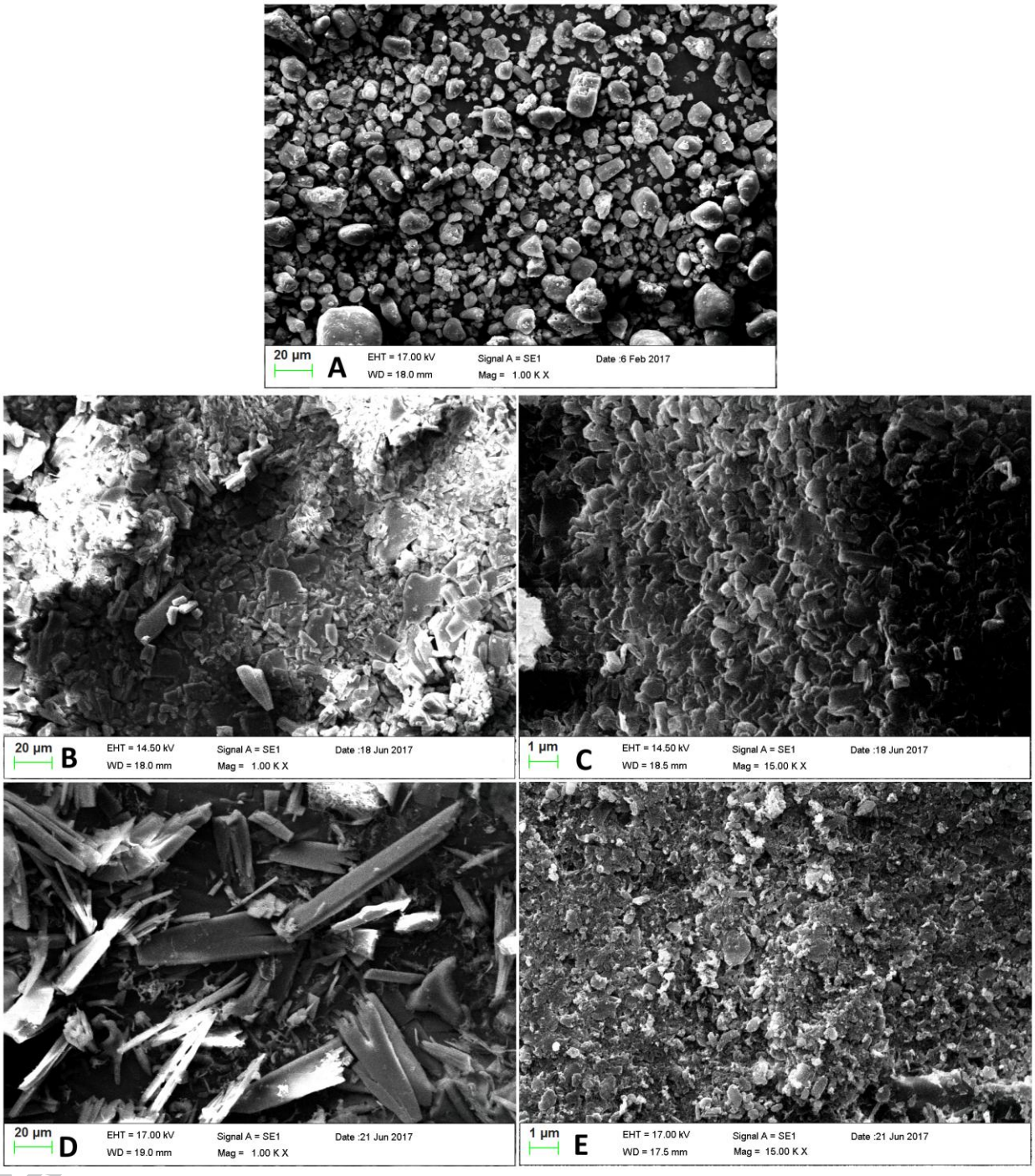
20 µm
A
EHT = 17.00 kV
WD = 18.0 mm
Signal A = SE1
Mag = 1.00 K X
Date :6 Feb 2017
20 µm
B
EHT = 14.50 kV
WD = 18.0 mm
Signal A = SE1
Mag = 1.00 K X
Date :18 Jun 2017
1 µm
C
EHT = 14.50 kV
WD = 18.5 mm
Signal A = SE1
Mag = 15.00 K X
Date :18 Jun 2017
20 µm
D
EHT = 17.00 kV
WD = 19.0 mm
Signal A = SE1
Mag = 1.00 K X
Date :21 Jun 2017
1 µm
E
EHT = 17.00 kV
WD = 17.5 mm
Signal A = SE1
Mag = 15.00 K X
Date :21 Jun 2017

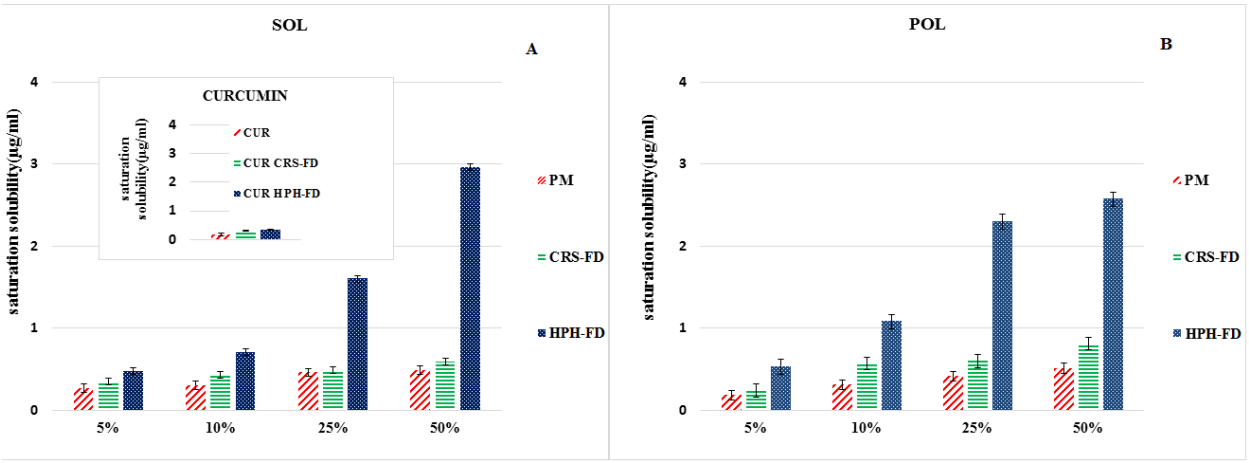

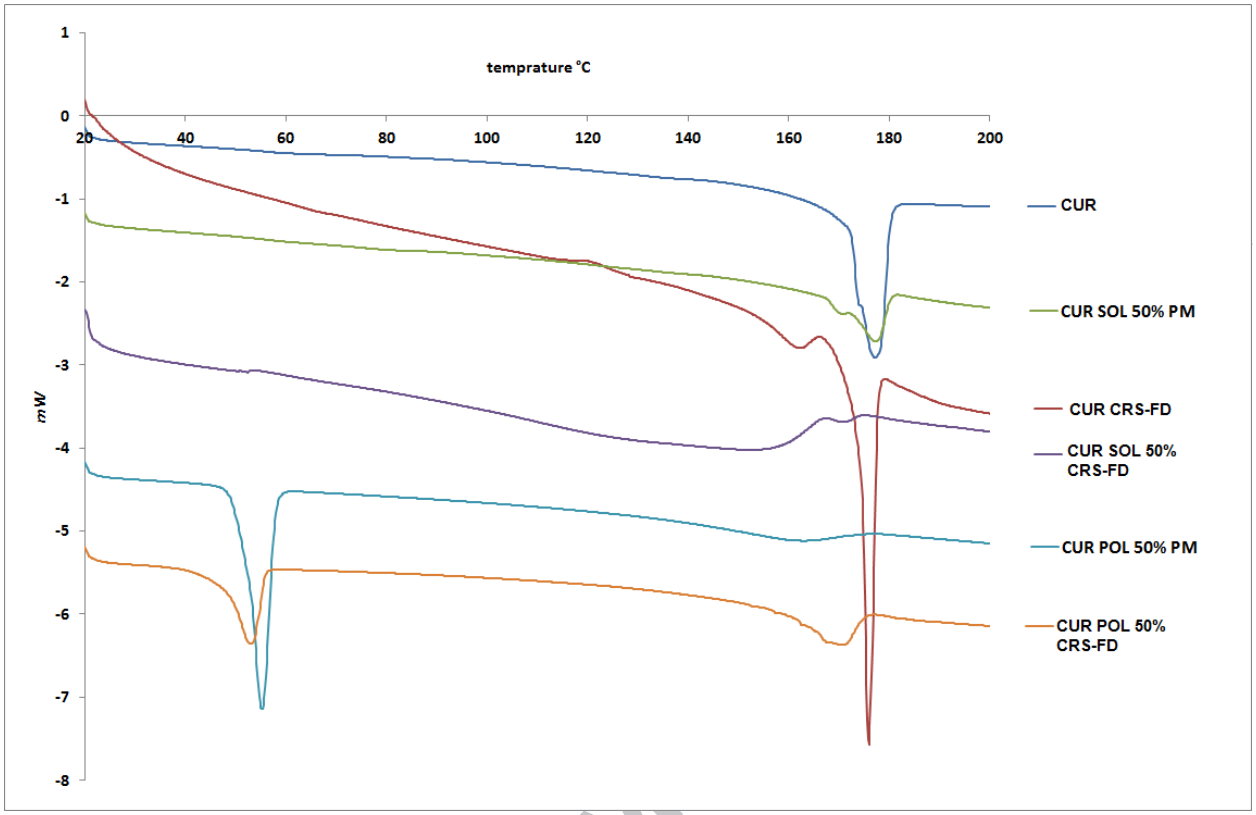

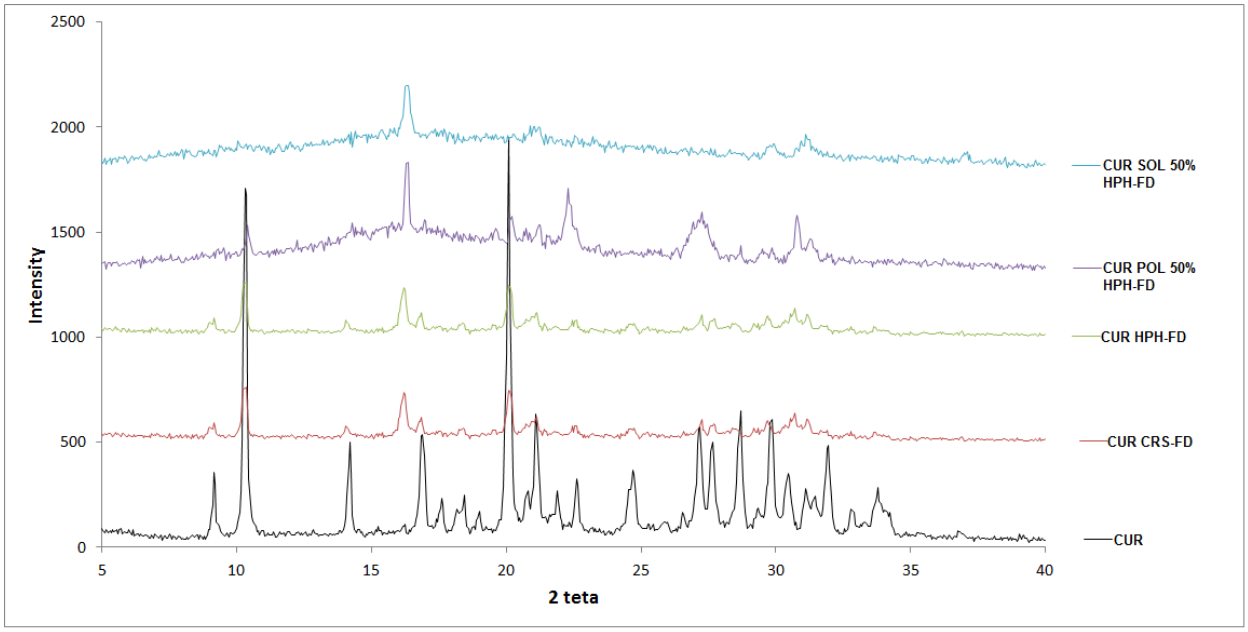

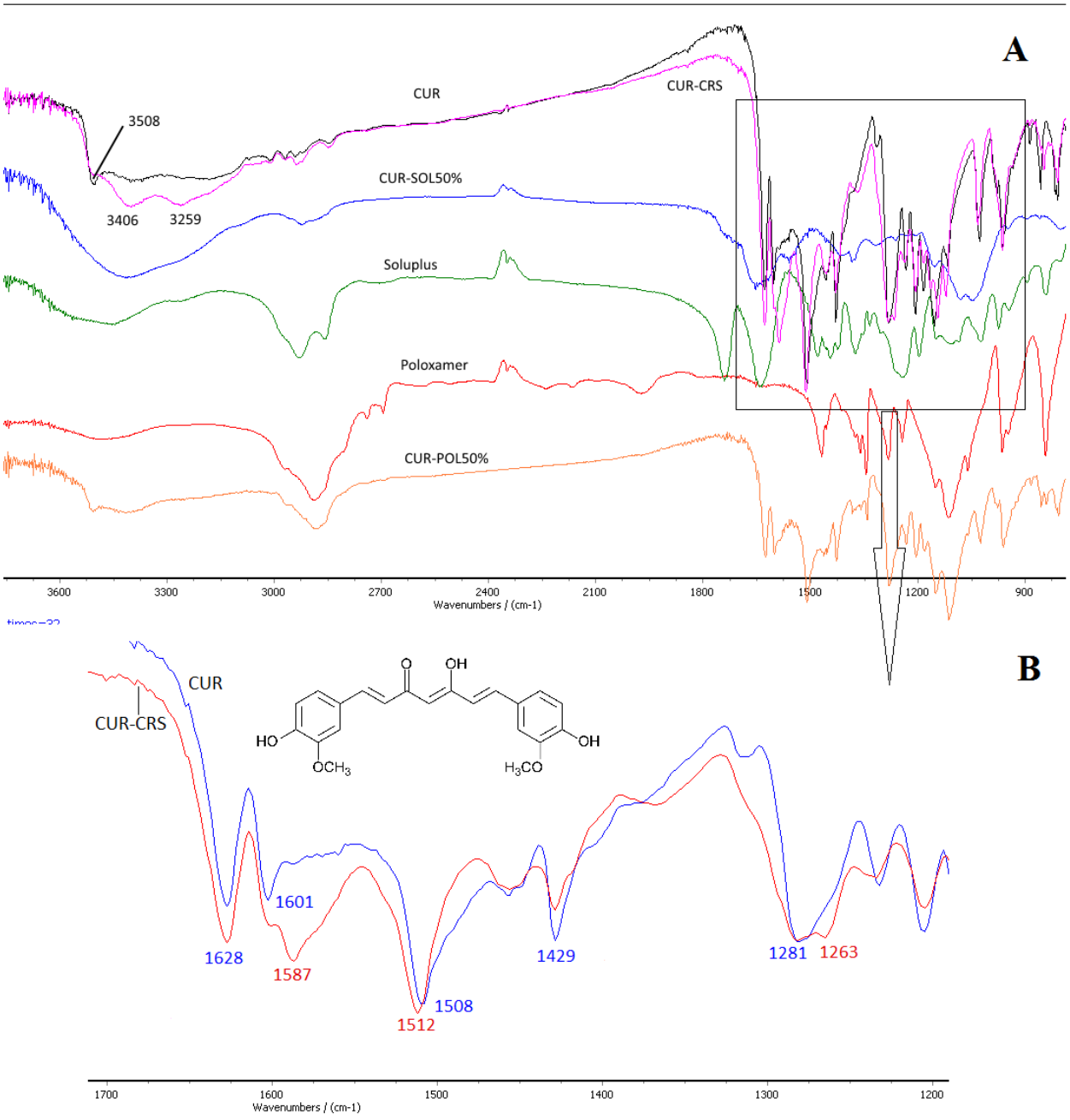

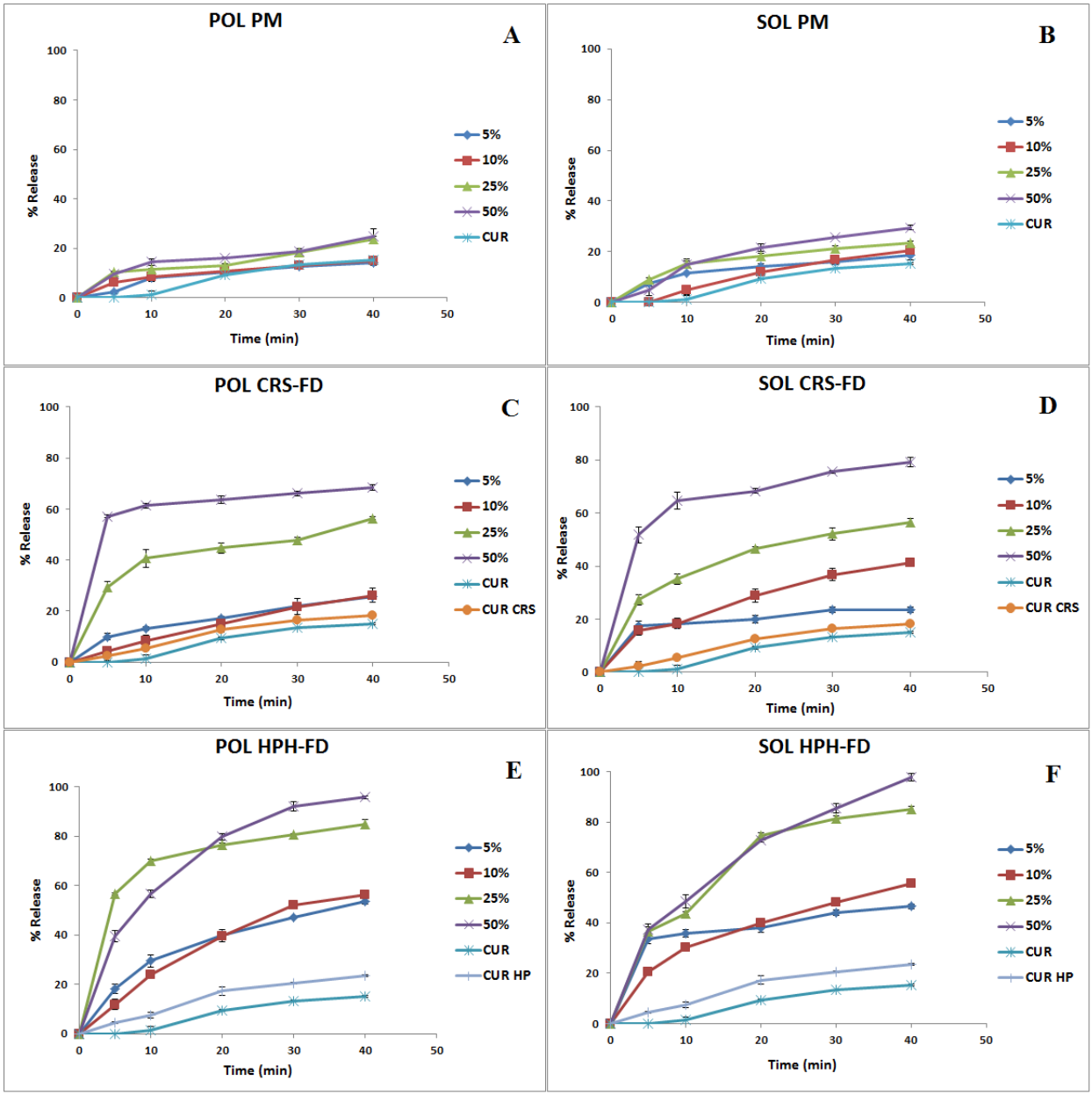

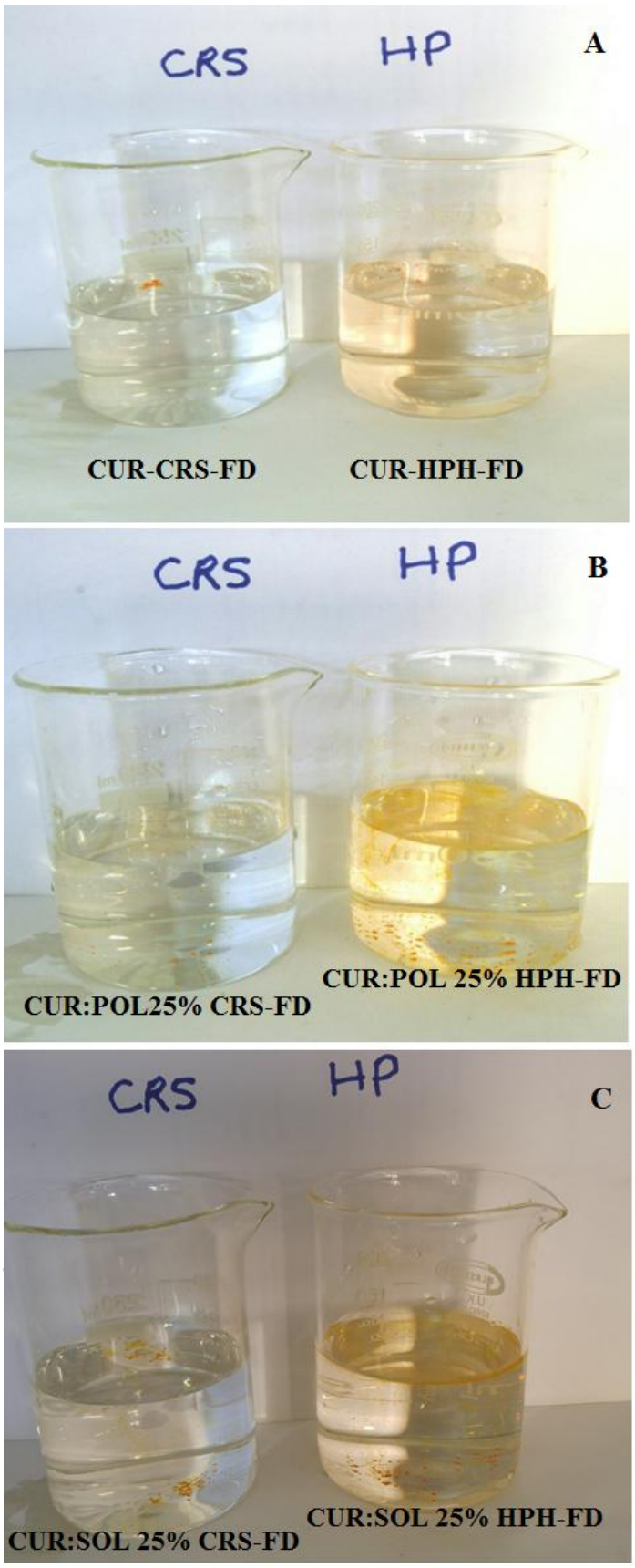
CRS
HP
A
CUR-CRS-FD
CUR-HPH-FD
CRS
HP
B
CUR:POL 25% HPH-FD
CUR:POL25% CRS-FD
CRS
HP
C
CUR:SOL 25% HPH-FD
CUR:SOL 25% CRS-FD